Cell Reports
Article

Tenascin-C Downregulates Wnt Inhibitor Dickkopf-1, Promoting Tumorigenesis in a Neuroendocrine Tumor Model

Falk Saupe,[1,2,3,4,12] Anja Schwenzer,[1,2,3,4,12] Yundan Jia,[1,2,3,4,5,12] Isabelle Gasser,[1,2,3,4] Caroline Spenlé,[1,2,3,4] Benoit Langlois,[1,2,3,4] Martial Kammerer,[1,2,3,4] Olivier Lefebvre,[1,2,3,4] Ruslan Hlushchuk,[6] Tristan Rupp,[1,2,3,4] Marija Marko,[1,2,3,4] Michael van der Heyden,[1,2,3,4] Gérard Cremel,[1,2,3,4] Christiane Arnold,[1,2,3,4] Annick Klein,[1,2,3,4] Patricia Simon-Assmann,[1,2,3,4] Valentin Djonov,[6] Agnès Neuville-Méchine,[7] Irene Esposito,[8] Julia Slotta-Huspenina,[8] Klaus-Peter Janssen,[9] Olivier de Wever,[10] Gerhard Christofori,[11] Thomas Hussenet,[1,2,3,4,*] and Gertraud Orend[1,2,3,4,5,*]

[1]Inserm U1109, MN3T Team, The Microenvironmental Niche in Tumorigenesis and Targeted Therapy, 3 Avenue Molière, 67200 Strasbourg, France
[2]Université de Strasbourg, 67000 Strasbourg, France
[3]LabEx Medalis, Université de Strasbourg, 67000 Strasbourg, France
[4]Fédération de Médecine Translationnelle de Strasbourg (FMTS), 67000 Strasbourg, France
[5]Institute of Biochemistry and Genetics, Department of Biomedicine, University of Basel, Extracellular Matrix Adhesion Team, Mattenstraße 28, 4058 Basel, Switzerland
[6]Institute of Anatomy, University of Bern, Baltzerstrasse 2, 3000 Bern, Switzerland
[7]Hospital Hautepierre, Department of Anatomy and Pathology, 1 Avenue Molière, 67200 Strasbourg, France
[8]Institute of Pathology and Anatomy, Technical University Munich, Trogerstrasse 18, 81675 München, Germany
[9]Department of Surgery Technical University Munich, Ismaningerstrasse 22, 81675 München, Germany
[10]Laboratory of Experimental Cancer Research, Department of Radiation Oncology and Experimental Cancer Research, Ghent University Hospital, De Pintelaan 185, 9000 Ghent, Belgium
[11]Institute of Biochemistry and Genetics, Department of Biomedicine, University of Basel, Switzerland, Tumor Biology Team, Mattenstraße 28, 4058 Basel, Switzerland
[12]These authors contributed equally to this work
*Correspondence: hussenetthomas@gmail.com (T.H.), gertraud.orend@inserm.fr (G.O.)
http://dx.doi.org/10.1016/j.celrep.2013.09.014

SUMMARY

The extracellular matrix molecule tenascin-C (TNC) is a major component of the cancer-specific matrix, and high TNC expression is linked to poor prognosis in several cancers. To provide a comprehensive understanding of TNC's functions in cancer, we established an immune-competent transgenic mouse model of pancreatic β-cell carcinogenesis with varying levels of TNC expression and compared stochastic neuroendocrine tumor formation in abundance or absence of TNC. We show that TNC promotes tumor cell survival, the angiogenic switch, more and leaky vessels, carcinoma progression, and lung micrometastasis. TNC downregulates Dickkopf-1 (*DKK1*) promoter activity through the blocking of actin stress fiber formation, activates Wnt signaling, and induces Wnt target genes in tumor and endothelial cells. Our results implicate DKK1 downregulation as an important mechanism underlying TNC-enhanced tumor progression through the provision of a proangiogenic tumor microenvironment.

INTRODUCTION

Manifestation of cancer requires many steps in which the microenvironment plays an essential role (Bissell and Labarge, 2005). A group of tumor cells with oncogenic mutations does not readily cause cancer, a phenomenon known as tumor dormancy (Aguirre-Ghiso, 2007). Angiogenesis presents an important step in awakening quiescent tumors and in driving their development into metastatic cancer (Almog, 2010). Tumor cells secrete soluble factors that attract endothelial cells (Kerbel, 2008). In addition, the extracellular matrix (ECM) constitutes a major fraction of cancer tissue and contributes to tumor angiogenesis and metastasis (Lu et al., 2012). An important component of the tumor-specific ECM is tenascin-C (TNC). TNC is known to promote malignant tumor progression and lung metastasis; yet, the underlying mechanisms are poorly understood (Midwood et al., 2011).

Because no stochastic and immune-competent in vivo model existed that would recapitulate the roles of TNC in tumor progression, we generated mouse lines with different expression levels of TNC (overexpression, wild-type, knockout) in the Rip1-Tag2 (RT2) model of pancreatic β-cell carcinogenesis (Hanahan, 1985). This model recapitulates multistage tumorigenesis as observed in most human cancers (Nevins, 2001; Pipas and Levine, 2001).

Here, we demonstrate that TNC promotes several steps in RT2 tumorigenesis including the angiogenic switch and lung micrometastasis. We provide a mechanistic basis showing that TNC downregulates expression of the soluble Wnt inhibitor Dickkopf-1 (DKK1) (Glinka et al., 1998) by blocking actin stress fiber formation and induces canonical Wnt signaling in tumor and endothelial cells. Our data suggest that DKK1 downregulation by TNC in tumor and stromal cells may provide a tumorigenesis signaling promoting microenvironment. Given that Wnt signaling is a crucial pathway driving angiogenesis and is activated by TNC, this pathway may play an important role in promoting tumor angiogenesis and metastasis by TNC. Thus, targeting TNC or its associated signaling pathways may represent a strategy to counteract tumor progression.

RESULTS

Tenascin-C Promotes Tumor Cell Survival, Proliferation, and Invasiveness

To address whether TNC potentially plays a role in the RT2 model (Hanahan, 1985), we determined TNC expression during RT2 tumorigenesis by immunofluorescence microscopy analysis (immunofluorescence [IF]). In normal pancreatic islets, TNC expression was undetectable, whereas a large fraction of hyperplastic and almost all angiogenic and tumorigenic islets expressed TNC (Figure S1A), suggesting a potential role of TNC during RT2 tumor progression. Therefore, we generated RT2 mice with overexpression of TNC (RT2/TNC) and a lack of TNC (RT2/TNCKO) (Figures S1B–S1G).

We performed tissue analysis to address whether ectopically expressed TNC had an effect on cell proliferation. We quantified the proportion of cells positive for phosphohistone-H3 by IF (Figure S2A) and observed that tumors of RT2/TNC mice exhibited 1.4-fold more proliferating cells than those from RT2 mice (Figure 1A) with a significant difference in hyperplastic islets (Figure S2C). Surprisingly, a similar difference was also seen in RT2/TNCKO tumors (Figures 1B and S2D). We also investigated a potential impact of ectopically expressed TNC on apoptosis by staining for cleaved caspase-3 (Figure S2B). RT2/TNC tumors exhibited 2.8-fold less apoptotic cells than RT2 wild-type tumors (Figures 1C and S2E). In contrast, apoptosis was unchanged in RT2/TNCKO tumors in comparison to RT2 controls (Figures 1D and S2F). However, no difference was seen in tumor multiplicity or tumor volume between genotypes (Figures S2G and S2H). Interestingly, upon tumor grading we observed that the frequency of carcinomas and the ratio of carcinomas over adenomas were higher in RT2/TNC mice (1.8) than in RT2 controls (0.8) (Figure 1E; Table S1). We conclude that transgenic TNC increases proliferation and survival in RT2/TNC mice and more importantly promotes tumor progression.

Tenascin-C Promotes the Angiogenic Switch and the Formation of Leaky and Abnormal Tumor Vessels

To address whether TNC has an effect on RT2 tumor angiogenesis, we isolated islets at the age of 8 weeks when the angiogenic switch takes place in a subset of neoplastic islets (Hanahan et al., 1996; Parangi et al., 1996) (Figure S2I). We noticed that the number of angiogenic islets was 2.4-fold higher in RT2/TNC and 2.9-fold lower in RT2/TNCKO mice in comparison to RT2 littermates (Figures 1F and 1G; Table S2). By quantification of CD31-positive endothelial cells (Figure S2J) in tumor sections of 12-week-old RT2 mice, we observed that the abundance of blood vessels was 2.6-fold higher and 1.6-fold lower in tumors of RT2/TNC and RT2/TNCKO mice, respectively, than in RT2 controls (Figures 1H and 1I).

We next addressed the question of a potential impact of TNC on vessel anatomy by scanning electron microscopy in Mercox corrosion casts of the tumor vasculature of multiple tumors of RT2 and RT2/TNC mice. Using this descriptive approach, we observed a highly aberrant vessel phenotype in some RT2/TNC tumors that has not been seen in RT2 tumors. These vessels were irregularly shaped, wider, discontinued, and bifurcated (see arrows), reminiscent of high vessel branching and/or leakage (Figures 1J and S2K). Because this approach is not suitable for quantitative determinations, we then studied vessel lining by pericytes using NG2 staining as readout for vessel functionality and maturation (Figure S2L). Despite more abundant pericytes in RT2/TNC tumors (Figure S2M), quantification of combined NG2 and CD31 staining signals revealed a 23.7% reduced ratio of NG2 over CD31 in RT2/TNC tumors (Figure 1K), which is indicative of a reduced pericyte coverage of vessels (Song et al., 2005). Finally, we assessed vessel functionality by analyzing fibrinogen (FBG) leakage in tumors upon PBS perfusion of tumor vessels followed by FBG staining (Huijbers et al., 2010) (Figure S2N). Whereas FBG leakage was slightly increased (close to significance, $p = 0.064$) in RT2/TNC over control tumors (Figures 1L and S2O), this analysis revealed a 1.7-fold significantly reduced FBG staining in RT2/TNCKO tumors over RT2 wild-type tumors (Figures 1M and S2P).

Altogether, our results suggest that, whereas TNC promotes the angiogenic switch and increases tumor blood vessel density, it decreases vessel coverage by pericytes and increases leakage, thus perturbing tumor vessel functionality.

Tenascin-C Increases Lung Micrometastasis

In a C57Bl/6 background, RT2 mice do not exhibit macroscopically visible metastasis. To address whether TNC had an effect on micrometastasis formation, we determined expression of insulin (as tumor cell-specific marker) in liver and lung tissue of tumor-bearing mice. Upon tissue staining, we detected cohorts of insulinoma cells within liver and lung tissue confirming their metastatic nature (Figures 2A and S3A). Hematoxylin and eosin (H&E) staining revealed their parenchymal localization. In a subset of mice, we compared quantification of insulin by immunostaining and quantitative RT-PCR (qRT-PCR). This showed a good correlation between both methods and indicates that quantification by qRT-PCR reflects parenchymal localization of micrometastasis rather than circulating tumor cells. We then analyzed a larger sample size of liver and lung tissue by qRT-PCR. Although we did not observe differences in liver tissue between genotypes (Figures S3B and S3C), *insulin* mRNA levels in lungs of RT2/TNC mice were 5.4-fold higher in comparison to lungs of RT2 controls (Figure 2B). Moreover, we observed 28.3-fold lower *insulin* mRNA levels in lungs of mice lacking TNC in comparison to control littermates carrying one TNC allele

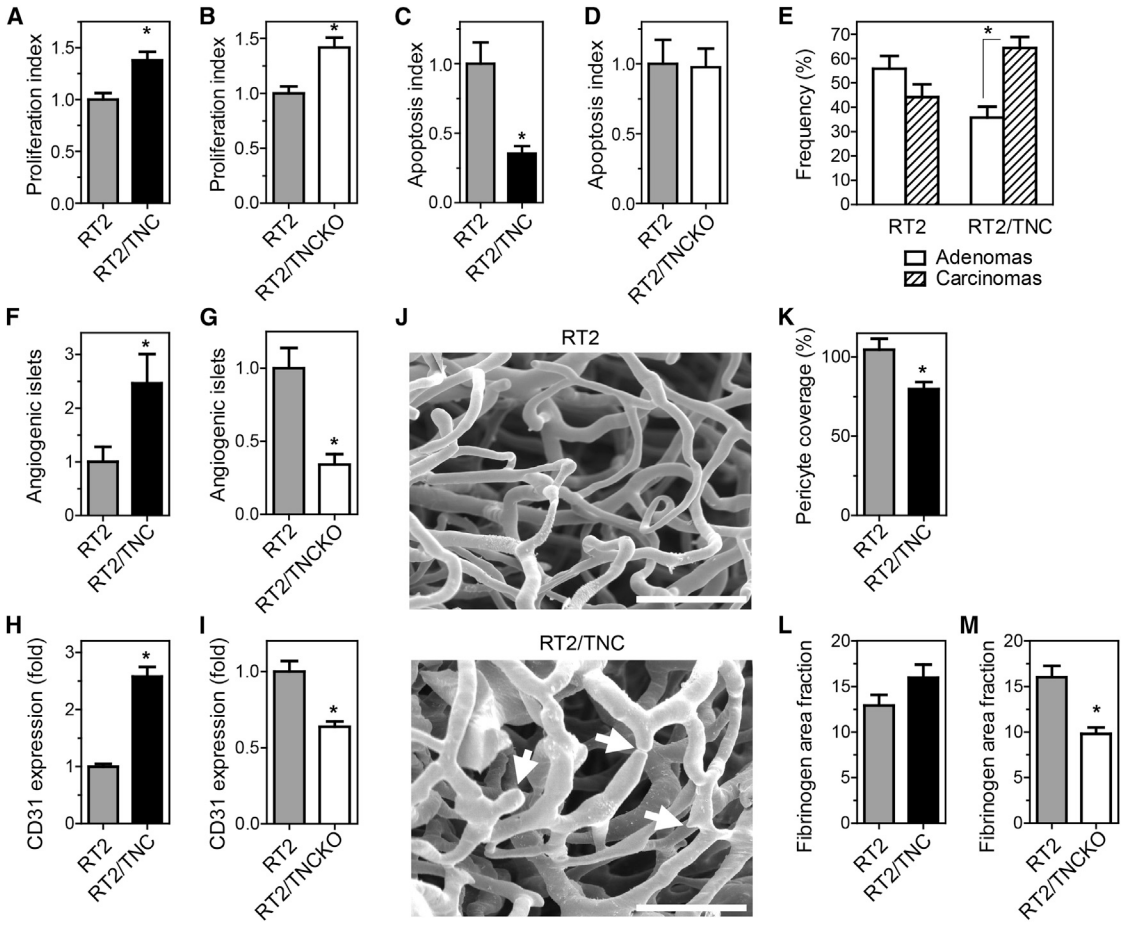

Figure 1. TNC Enhances Proliferation, Survival, and Tumor Progression in RT2 Tumors

(A and B) Quantification of proliferating cells in tumor sections as PH3-positive nuclei in 12-week-old mice. (A) RT2 (n = 9 mice, n = 150 islets), RT2/TNC (n = 8, n = 140). (B) RT2 (n = 6, n = 131) and RT2/TNCKO (n = 6, n = 137).

(C and D) Quantification of apoptotic cells as cleaved caspase-3-positive cells in tumor sections of 12-week-old mice. (C) RT2 (n = 6 mice, n = 84 islets), RT2/TNC (n = 8, n = 123). (D) RT2 (n = 4, n = 95) and RT2/TNCKO (n = 4, n = 83).

(E) Tumor grading into adenoma or invasive carcinoma (H&E-stained tumor sections) of RT2 tumors (n = 26 mice, 78 adenomas, 79 carcinomas) and RT2/TNC (n = 22, 44 adenomas, 76 carcinomas). See Table S1.

(F and G) Number of angiogenic islets per mouse normalized to RT2 controls. See Table S2.

(H and I) Tumor blood vessel quantification upon CD31 staining of tumor sections from 12-week-old mice as CD31-positive area fraction per tumor normalized to RT2 controls. (H) RT2 (n = 6 mice, n = 34 tumors, 203 images) and RT2/TNC (n = 4, n = 17, 106 images). (I) RT2 (n = 3, n = 71) and RT2/TNCKO (n = 3, n = 111).

(J) Morphology of the tumor vasculature in Mercox perfusion casts from 12-week-old RT2 and RT2/TNC mice. Arrows point at break point, branching, and constriction. Scale bars, 50 μm.

(K) Pericyte coverage of tumor blood vessels upon quantification of the ratio of NG2 over CD31 staining signals. RT2 (n = 6 mice, n = 155 tumors) and RT2/TNC (n = 8, n = 204).

(L and M) Quantification of tumor blood vessel leakage upon fibrinogen staining of tumor sections from 12-week-old mice as fibrinogen-positive area fraction per tumor. (L) RT2 (n = 5 mice, n = 62 tumors) and RT2/TNC (n = 3, n = 50). (M) RT2 (n = 4, n = 60) and RT2/TNCKO (n = 5, n = 125). Error bars represent SEM. *$p < 0.05$. See also Figures S1 and S2 and Tables S1 and S2.

(Figure 2C). Our results suggest that in the RT2 model TNC does not affect liver metastasis but increases lung micrometastasis formation.

TNC Expression Correlates with Low Dkk1 Levels and Increases Wnt Target Gene Expression

Because we had noticed downregulation of the Wnt pathway inhibitor DKK1 in T98G glioblastoma cells cultivated on a TNC-containing substratum (Ruiz et al., 2004), we assessed a potential impact of TNC on Dkk1 expression in tumors of the different RT2 genotypes. By qRT-PCR, we noticed that 12 times more RT2/TNC tumors (46.1%) lacked *Dkk1* expression as compared to RT2 controls (3.7%) (Figure 3A). In RT2/TNC tumors with detectable *Dkk1* expression, the levels were 16.1-fold reduced in comparison to RT2 controls (Figure 3B). In contrast, *Dkk1* levels were 2.6-fold higher in tumors lacking TNC as compared to control tumors with one TNC allele (Figure 3C). These observations demonstrate an inverse correlation between TNC and

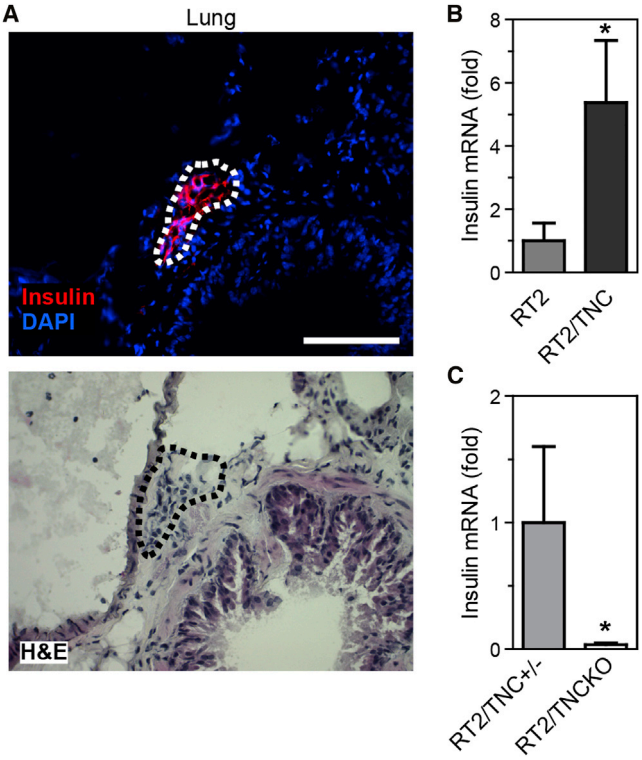

Figure 2. Lung Micrometastasis in RT2 Mice

Insulin expression in a lung RT2 micrometastasis (A) and quantification by qRT-PCR (B and C). (A) Detection of metastasized insulin-positive tumor cells in lung parenchyma (RT2 mouse) by immunostaining (upper panel) and H&E staining (adjacent section, lower panel). Scale bar 50 μm. Detection of insulin expression in RT2 (9/24) and RT2/TNC mice (11/24) (B) and in RT2/TNC$^{+/-}$ (8/13) and RT2/TNCKO littermates (4/13) (C). Error bars represent SEM. *p < 0.05. See also Figure S3.

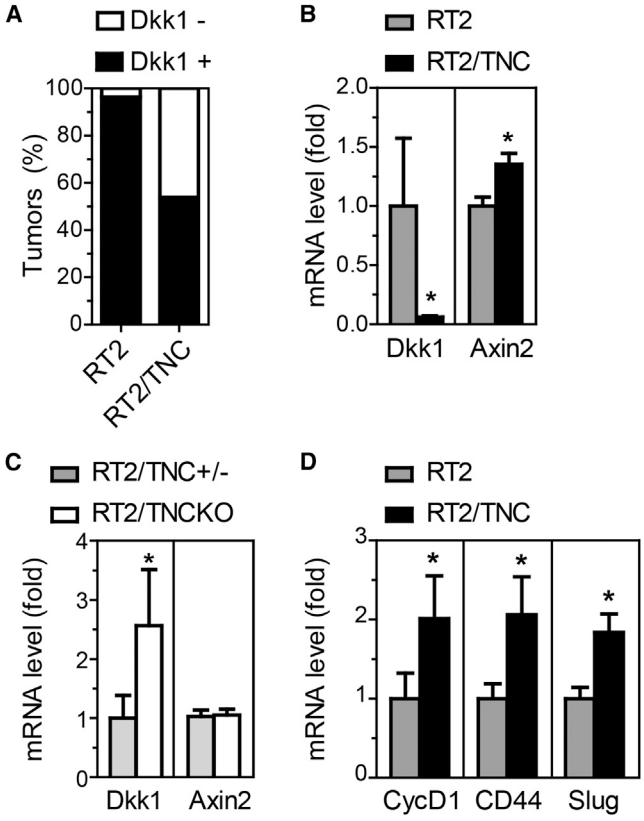

Figure 3. Dkk1 Expression in RT2 Tumors

(A) Tumors were stratified according to *Dkk1* levels, as Dkk1 expressing (Dkk1^{+}) or not expressing (Dkk1^{-}). *Dkk1* was found to be expressed in 26 of 27 RT2 tumors and in 7 of 13 RT2/TNC tumors. Difference between genotypes, $p < 0.05$.

(B) Dkk1 expression was largely reduced in those RT2/TNC tumors with detectable *Dkk1* expression. *Axin2* expression was enhanced in RT2/TNC tumors.

(C) In RT2/TNCKO tumors (15 of 24 tumors were Dkk1 positive) Dkk1 expression was higher compared to RT2/TNC$^{+/-}$ tumors (16 of 23 tumors were Dkk1 positive). Axin2 expression was not changed.

(A–C) *Dkk1* and *Axin2* expression was analyzed by qRT-PCR.

(A–D) Wnt target gene expression in all RT2/TNC and RT2/TNCKO tumors (A–C) or in small differentiated tumors (D), see Table S3. Error bars represent SEM. *p < 0.05.

Dkk1 expression and suggest that TNC may activate Wnt signaling through *Dkk1* repression. To address this possibility, we determined the expression of Wnt target genes by qRT-PCR. We observed an increased expression of the bona fide Wnt signaling target *Axin2* (1.4-fold) in RT2/TNC tumors (Figure 3B), whereas its expression was unchanged in RT2/TNCKO tumors (Figure 3C). This result suggested that ectopic TNC expression induced Wnt signaling, prompting us to analyze expression of other Wnt target genes. Indeed, other Wnt targets such as *Cyclin D1* (2.0-fold), *CD44* (2.0-fold), and *Slug* (1.8-fold) were upregulated in small differentiated tumors of RT2/TNC mice (Figure 3D; Table S3). These results suggest that TNC may contribute to Wnt signaling activation in RT2/TNC tumors through downregulation of the inhibitor Dkk1.

Wnt Activation and DKK1 Inhibition by TNC in Cultured Tumor and Stromal Cells

We then designed in vitro experiments to evaluate a potential Wnt activation by TNC involving DKK1. We used a Wnt reporter (TOPFlash) assay where the expression of the *luciferase* gene is driven by a promoter containing TCF/LEF binding sites. Upon growth of Wnt-3A-stimulated osteosarcoma KRIB cells on a TNC-containing substratum, we observed a 3.5-fold increased Wnt reporter activity (Figure 4A) and a 2.0-fold increased expression of *AXIN2* (Figure 4B), demonstrating that TNC activates the Wnt pathway.

Next, we determined whether TNC affects secretion of soluble factors regulating Wnt signaling in KRIB cells. Therefore, we measured Wnt reporter activity of Wnt-3A-stimulated KRIB cells upon incubation with conditioned medium (CM) from the same cells previously grown on fibronectin (FN) or FN/TNC and observed that, indeed, Wnt activity was higher with CM from cells cultured in the presence of TNC (Figure 4C). These results suggest that TNC activates Wnt signaling through modulating the secretion of activators or inhibitors of the Wnt pathway.

To address whether Wnt inhibitors are regulated by TNC, we investigated their expression by qRT-PCR in cells grown on FN/TNC and FN. Although some inhibitors (*DKK4* and *SFRP2*)

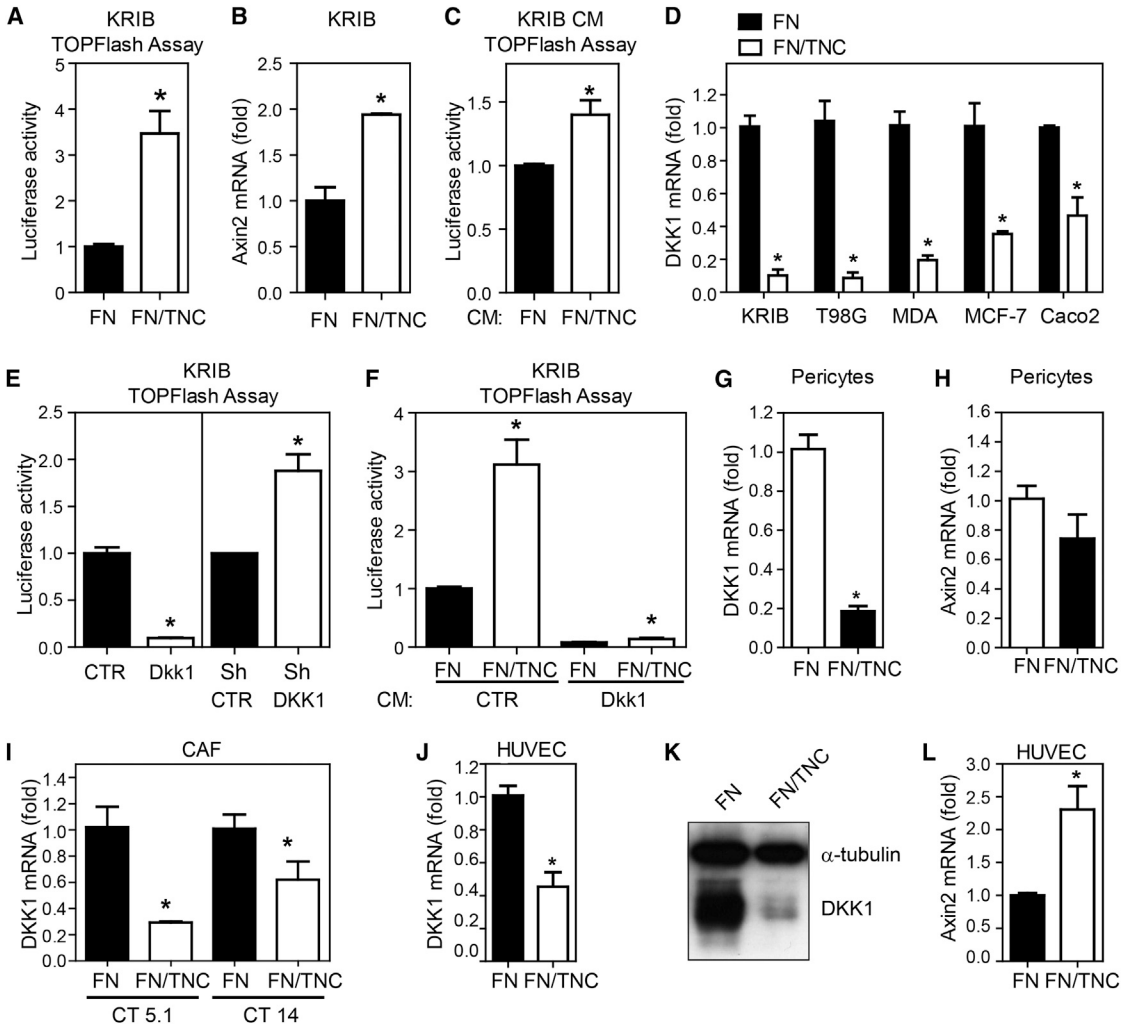

Figure 4. TNC Leads to DKK1 Downregulation and Wnt Signaling Activation in Tumor Cells and Endothelial Cells

(A–C) Enhanced Wnt signaling in Wnt-3A-treated KRIB cells by TNC. TOPFlash activity of cells grown on FN or FN/TNC for 48 hr (A) or treated for 48 hr with Wnt-3A CM and CM of cells grown on FN or FN/TNC (C). (B) *AXIN2* mRNA levels (qRT-PCR, 5 hr).

(D) *DKK1* expression (qRT-PCR, 24 hr) in the indicated tumor cell lines (KRIB, T98G, MDA-MB-435 [MDA], MCF-7, and Caco2) on FN/TNC is represented relative to its expression on FN.

(E) Cell autonomous impact of low (knockdown) and high (overexpression) DKK1 on Wnt signaling as analyzed by TOPFlash activity after 48 hr.

(F) Repression of TNC-mediated Wnt signaling activation by Dkk1. TOPFlash luciferase activity was performed as in (A) except the addition of CM from KRIB control or Dkk1-overexpressing cells after 5 hr of cell seeding on the indicated substrata. Note that the TNC-containing substratum still induced Wnt signaling activity in presence of Dkk1-containing CM, but to a lesser extent (1.8-fold) than in the control conditions (3.1-fold).

(G–I) *DKK1* and *Axin2* mRNA levels in pericytes (G and H) and two human colorectal-cancer-derived CAF primary lines (I) seeded on FN or FN/TNC (5 hr). TNC leads to downregulation of *DKK1* in pericytes and CAFs (G and I), but *AXIN2* expression remains unchanged in pericytes (H).

(J–L) Enhanced Wnt signaling by TNC in HUVECs. qRT-PCR for DKK1 and AXIN2 (5 hr) (J and L) and DKK1 immunoblotting (24 hr) (K). Data from three independent experiments (except D: MCF-7 and Caco2 cell lines, one and two experiments, respectively; and I: two experiments) are shown as mean ± SEM. *$p < 0.05$.

See also Figure S4.

were not expressed, no consistent effect of TNC was observed on the expression of other analyzed Wnt inhibitors (*DKK2*, *DKK3*, *SFRP1*, *SFRP3*, *SFRP4*) in KRIB, T98G, and MDA-MB435 cells (Figure S4A). In contrast, we observed a robust downregulation of *DKK1* in all five analyzed tumor cell lines of different origin after 24 hr on the TNC-containing substratum (Figures 4D and S4A). DKK1 downregulation was observed at both RNA and protein levels, with a fast (5 hr) and long-lasting (up to 12 days) effect in T98G cells (Figures S4B and S4C).

To determine whether modulation of DKK1 expression contributes to TNC-dependent Wnt signaling in KRIB cells, TOPFlash activity was measured upon overexpression and knockdown of DKK1, respectively (Figures S4D–S4G). Indeed, activity of the Wnt signaling reporter was DKK1 dependent because it was increased upon DKK1 knockdown and decreased upon Dkk1 overexpression (Figure 4E) and was repressed by Dkk1-containing CM in a dose-dependent manner (Figure S4H). When KRIB cells were incubated with Dkk1 CM on

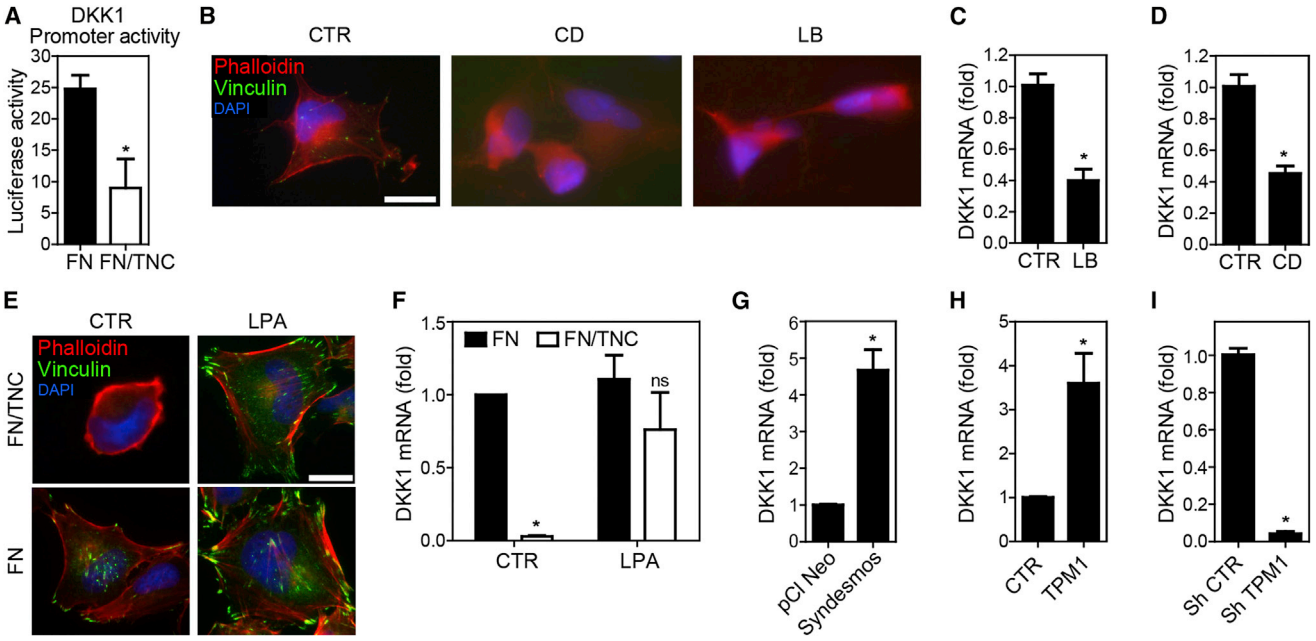

Figure 5. Mechanism of DKK1 Downregulation

(A) Reduced *DKK1* promoter activity by TNC. *DKK1* promoter driven luciferase activity in T98G cells is shown upon growth for 48 hr on the indicated substrata.

(B and E) Phalloidin (red) and vinculin (green) stainings of serum-starved T98G cells upon CTR, CD (2 μM), or LB (5 μM) treatment for 3 hr (B). Nuclei are stained in blue (DAPI). Scale bar 20 μm.

(C and D) *DKK1* mRNA levels in serum-starved T98G upon LB (5 μM, 3 hr) (C) or CD (2 μM, 3 hr) (D) treatment.

(E) IF staining of T98G cells upon control or LPA (30 μM) treatment. Serum-starved T98G were plated on fibronectin (FN) or fibronectin/tenascin-C (FN/TNC), and after 1 hr LPA was added for 4 hr. Although cells are poorly spread under control conditions on FN/TNC (no actin stress fibers, few focal adhesions), LPA treatment restored cell spreading associated with the formation of focal adhesions and actin stress fibers. Scale bar, 20 μm.

(F) *DKK1* mRNA expression determined by qRT-PCR upon treatment with 30 μM LPA. LPA restores *DKK1* expression on FN/TNC.

(G–I) *DKK1* mRNA expression determined by qRT-PCR upon ectopic expression of chicken syndesmos (G) and mouse TPM1 (H) or upon knockdown of TPM1 (I). Syndesmos or TPM1 overexpression induces *DKK1* mRNA expression, whereas TPM1 knockdown leads to *DKK1* downregulation.

Data are shown as mean ± SEM. *$p < 0.05$. See also Figure S5.

FN/TNC and FN, Wnt reporter activity was largely reduced (Figure 4F), suggesting that TNC-induced repression of DKK1 facilitates Wnt pathway activation.

Next, we determined whether stromal cells also downregulated DKK1 on a TNC substratum. Therefore, *DKK1* expression was determined in two monocytic/macrophage cell lines, primary human brain pericytes, two colorectal cancer derived carcinoma associated fibroblasts (CT5.1, CT14), and human umbilical vein endothelial cells (HUVECs) upon growth on FN/TNC and FN. We noticed that in contrast to the two macrophage lines that did not at all express *DKK1*, pericytes (5-fold), CAFs (3.0- and 1.6-fold), and HUVECs (2.2-fold) significantly downregulated DKK1 mRNA (Figures 4G, 4I, and 4J) and protein (Figure 4K) on a TNC substratum. Whereas *Axin2* expression was not affected in pericytes (Figure 4H), *Axin2* mRNA was 2.3-fold increased in HUVECs on FN/TNC in comparison to FN (Figure 4L). Altogether, our results show that TNC induces downregulation of DKK1 in tumor and stromal cells and activates Wnt signaling in tumor and endothelial cells.

Mechanism of DKK1 Downregulation by TNC

First, we determined whether *DKK1* mRNA stability is substratum dependent. Therefore, T98G cells were treated with the RNA polymerase II inhibitor Actinomycin D, but DKK1 mRNA levels were equally low in cells on FN and FN/TNC, suggesting that *DKK1* is not regulated by mRNA stabilization (Figure S5A). Next, we addressed whether TNC downregulates DKK1 at transcriptional level. Therefore, we performed reporter assays by measuring luciferase activity under control of a 3.2 kb *DKK1* promoter sequence. Indeed, we observed a 2.5-fold reduced *DKK1* promoter activity in cells grown for 48 hr on a TNC-containing substratum (Figure 5A).

Because TNC blocks actin stress fiber formation (Huang et al., 2001; Midwood et al., 2004; Murphy-Ullrich et al., 1991; Orend et al., 2003), we investigated whether disruption of the actin cytoskeleton has an impact on *DKK1* mRNA levels. Treatment with Latrunculin B (LB) and Cytochalasin D (CD) disrupted actin stress fibers and focal adhesions and, importantly, reduced *DKK1* expression (Figures 5B–5D). To address the converse whether more actin stress fibers stimulate *DKK1* expression, we treated KRIB and T98G cells with lysophosphatidic acid (LPA) and observed an increased and dose-dependent *DKK1* mRNA expression similar to serum response factor (SRF), a known actin stress fiber-regulated gene (Gineitis and Treisman, 2001; Spencer and Misra, 1999) (Figures S5B–S5F). Moreover, LPA (30 μM) restored cell spreading, actin stress fibers, and focal

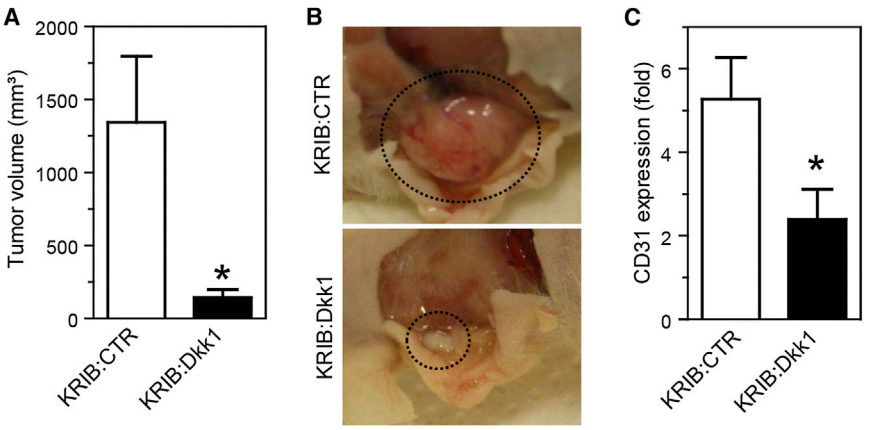

Figure 6. Dkk1 Overexpression Inhibits Osteosarcoma Growth and Angiogenesis

(A) Mean tumor volume of control (CTR, n = 10) and Dkk1-overexpressing (n = 9) KRIB tumors upon subcutaneous injection of the corresponding cells into nude mice.

(B) Representative tumor images.

(C) Tumor microvessel density, as determined by CD31 staining and quantification, was 2.2-fold reduced in KRIB:Dkk1 tumors (n = 8) as compared to control KRIB tumors (n = 10).

Error bars represent SEM. *p < 0.05. See also Figure S6.

adhesions in T98G cells on a FN/TNC substratum and most importantly largely restored *DKK1* levels on this substratum to that on FN (Figures 5E and 5F). Because LPA can trigger RhoA signaling (Mills and Moolenaar, 2003), and RhoA expression (Lange et al., 2007) and function (Wenk et al., 2000) are impaired by TNC, we determined whether overexpression of a constitutively active (CA) RhoA molecule impacts on *DKK1* expression. Whereas, CA-RhoA increased SRF target gene expression (Figures S5G–S5J), it did not alter *DKK1* expression (Figures S5K and S5L), suggesting that LPA triggers *DKK1* expression by a RhoA-independent pathway.

Because tropomyosin-1 (TPM1) and syndesmos overexpression bypass the cell adhesion blocking and actin stress-fiber-disrupting effect of TNC on a FN/TNC substratum (Lange et al., 2008), we determined whether ectopic expression of syndesmos and TPM1 have an impact on *DKK1* expression. Whereas shTPM1 blocked *DKK1* expression, overexpression of syndesmos and TPM1 increased *DKK1* mRNA levels to 4.7- and 3.6-fold, respectively (Figures 5G–5I and S5M–S5P).

Altogether, these results demonstrated that *DKK1* expression is regulated at the promoter level and that actin stress fibers and focal adhesion signaling drive *DKK1* transcription independently of RhoA. We conclude that TNC downregulates *DKK1* transcription by blocking focal adhesion and actin stress fiber formation.

Repression of Tumor Angiogenesis by DKK1

As we observed that TNC promotes tumor angiogenesis and downregulates *DKK1* expression, we addressed whether DKK1 impacts on tumor angiogenesis in xenografted tumors of KRIB cells with different DKK1 levels. We found that upon Dkk1 overexpression (Figure S6A) tumors were significantly smaller (Figure 6A) and pale (Figure 6B). Quantification of microvessel density upon CD31 staining revealed that Dkk1-overexpressing tumors were less vascularized (Figure 6C), suggesting that Dkk1 overexpression impaired tumor angiogenesis. In addition, conditioned medium from KRIB cells overexpressing Dkk1 inhibited HUVEC tubulogenesis on Matrigel in vitro (Figure S6D). We addressed whether Dkk1 potentially had an impact on tumor growth through inhibiting tumor cell proliferation and found no statistically significant difference in proliferation in cultured cells or in the tumors with elevated Dkk1 levels (Figures S6B and S6C).

Because Dkk1 influenced proliferation of tumor cells neither in vitro nor in vivo, our data suggest that Dkk1 overexpression impairs angiogenesis and thereby inhibits KRIB tumor growth. Because DKK1 blocks angiogenesis in a VEGFA context (Min et al., 2011), we investigated whether full-length TNC binds VEGFA. Indeed, by surface plasmon resonance we observed a dose-dependent binding of VEGFA to TNC (Figure S7), extending data on binding of VEGFA to the fifth FNIII domain in TNC (De Laporte et al., 2013) by providing a K_d of 2.7×10^{-7} M, which is in the range of a VEGFA/glycosaminoglycan interaction (2.4×10^{-8} M) (Wu et al., 2009).

TNC Expression in Human Insulinomas

As we demonstrated a tumor-promoting effect of TNC in the murine RT2 insulinoma model, we assessed a potential clinical relevance by determining TNC expression in human insulinomas using qRT-PCR and immunohistochemical staining of patient tumor tissue. Of note, insulinomas are rare and most are benign, yet a few (10%–15%) metastasize to lymph nodes and liver (Metz and Jensen, 2008). At RNA level, we found that *TNC* expression was detectable in all analyzed human insulinomas (Figure 7A). Most importantly, we observed the highest *TNC* expression levels (3/14) in tumors from patients with metastasis to liver or lymph nodes (Figures 7A and 7B), suggesting that a high TNC expression correlates with metastasis formation in human insulinomas.

DISCUSSION

We have used the RT2 model of multistage pancreatic β-cell tumorigenesis with abundant and no TNC expression to obtain a better understanding of TNC contribution to tumor progression and we have observed multiple effects. Enhanced TNC levels in TNC transgenic RT2 mice correlate with an increase in tumor cell proliferation and survival, carcinoma formation, angiogenesis, and lung micrometastasis. On the contrary, the absence of TNC results in reduced angiogenesis and lung micrometastasis. These results confirm a crucial role of TNC in tumor progression as has been suspected in human cancer.

There is much evidence for an important role of TNC in promoting tumor angiogenesis (Midwood et al., 2011). However, despite the fact that TNC has been extensively investigated for almost three decades (Chiquet-Ehrismann et al., 1986), it is not

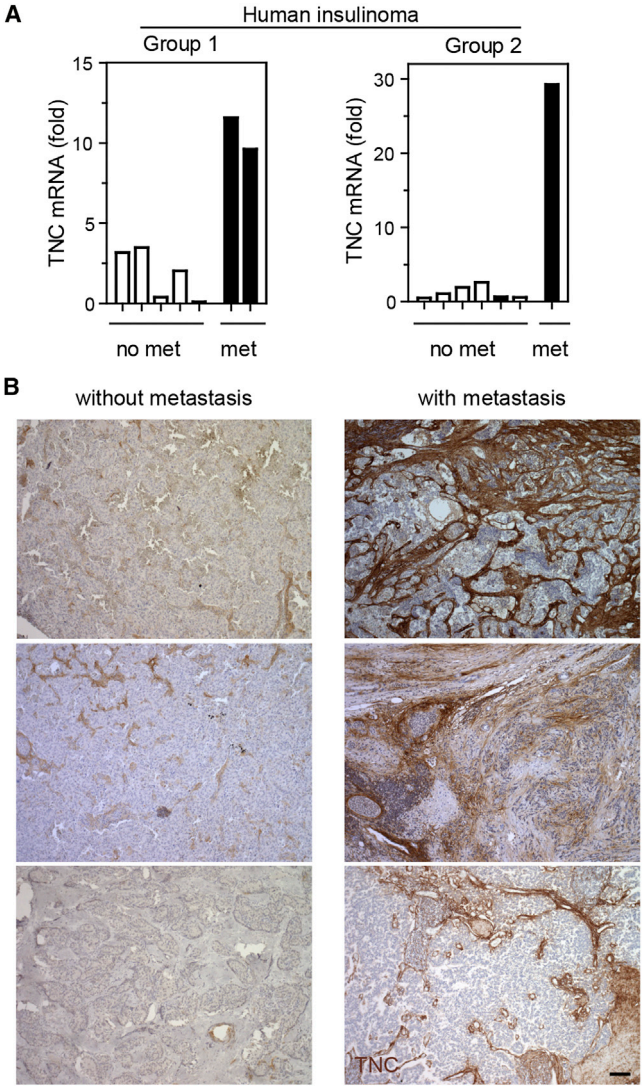

Figure 7. TNC Expression Correlates with Metastasis Formation in Human Insulinomas

(A) *TNC* mRNA expression was determined by qRT-PCR in two patient groups (group 1, Munich cohort; group 2, Strasbourg cohort) and is displayed as relative expression upon normalization to *GAPDH*. Upon combining data of the two groups, *TNC* expression in patients with metastasis is increased over that in patients without metastasis ($p < 0.05$).

(B) TNC expression was determined by IHC in all tumors of the two groups of insulinomas. Representative pictures of the three metastatic and three non-metastatic insulinomas are shown. Scale bar, 100 μm.

resolved how TNC impacts tumor angiogenesis at the molecular level. Whereas TNC can have stimulatory effects on endothelial cell migration, conflicting reports exist concerning its impact on tubulogenesis. A proangiogenic effect of TNC linked to VEGFA expression was seen in human melanoma xenografts implanted into immune-compromised mice lacking TNC (Tanaka et al., 2004). Of note, in the RT2/TNC tumors we did not observe an increased *VEGFA* expression (M.K., F.S., G.O., unpublished data). Our study addresses the role of TNC on tumor angiogenesis systematically by using a stochastic genetic tumor model with an intact immune system. Here, we investigated the angiogenic switch, tumor blood vessels, and their functionality. Most importantly, our study shows that TNC promotes the angiogenic switch, a rate-limiting step along tumor progression (Hanahan and Folkman, 1996), and the abundance of endothelial cells. However, TNC seems to impair vessel functionality because tumor vessels of RT2/TNC mice are morphologically aberrant and less covered by pericytes. Moreover, vessels in RT2 tumors lacking TNC are less leaky than those with TNC, suggesting a role of TNC in the formation of more but less functional tumor vessels.

We have identified DKK1 as an important TNC target in RT2 tumors. Our in vivo and in vitro results suggest that TNC promotes tumor progression involving DKK1 downregulation and activation of Wnt signaling. First, the *TNC* copy number inversely correlates with *DKK1* expression in RT2 tumors, and a TNC substratum downregulates *DKK1* expression in tumor and several stromal cell types (CAFs, pericytes, and endothelial cells). Second, Wnt signaling is increased by TNC in the RT2 model and in cultured endothelial and tumor cells. Third, TNC-induced Wnt activation is reduced in tumor cells by DKK1. Finally, downregulation of *DKK1* by TNC may be a key event because no other major Wnt inhibitor is consistently regulated by a TNC-containing substratum (our data; Ruiz et al., 2004).

Several transcriptional regulators, epigenetic silencing, and tissue tension were shown to regulate DKK1 expression (Aguilera et al., 2006; Barbolina et al., 2013; Liao et al., 2008; Menezes et al., 2012; Pendás-Franco et al., 2008; Zhou et al., 2012). Here, we demonstrate that TNC downregulates *DKK1* expression by promoter inhibition. Because TNC blocks actin stress fiber formation (Huang et al., 2001; Midwood et al., 2004; Murphy-Ullrich et al., 1991; van Obberghen-Schilling et al., 2011), we investigated whether *DKK1* expression is regulated by the actin polymerization state and demonstrated that TPM1 antisense and drug-induced disruption of the actin cytoskeleton reduced *DKK1* mRNA levels. On the contrary, enforcing actin polymerization and stress fiber formation by overexpression of syndesmos, bridging integrin $\alpha5\beta1$ and syndecan-4 in focal adhesions (Bass and Humphries, 2002), largely increased *DKK1* expression. We further showed that LPA rescued focal adhesion and actin stress fiber formation and cell spreading on FN/TNC, which we linked to restored *DKK1* expression in a RhoA-independent manner. How TNC downregulates *DKK1* expression at promoter level is currently unknown and requires further investigation, but it does not appear to be exclusively dependent on the SRF cotranscription factor MKL1 that is regulated by actin polymerization (Miralles et al., 2003) (A.S. and G.O., unpublished data). Previously, it was shown that a stiffened collagen substratum, implicating integrin adhesion signaling (Levental et al., 2009), induces *DKK1* downregulation in several cell types including endothelial cells (Barbolina et al., 2013). Here, we report a mechanism whereby TNC blocks *DKK1* transcription through disruption of actin stress fibers.

The role of DKK1 in developmental and tumor angiogenesis appears to be context dependent, because DKK1 can produce pro- and antiangiogenic effects (Aicher et al., 2008; De Langhe et al., 2005; Min et al., 2011; Oh et al., 2012; Reis

et al., 2012; Smadja et al., 2010). Interestingly, the growth factor context seems to be particularly critical for the outcome, because, for example, DKK1 promotes basic fibroblast-growth-factor-induced angiogenesis (Aicher et al., 2008; Reis et al., 2012; Smadja et al., 2010) but blocks VEGFA-induced (Min et al., 2011) angiogenesis in Matrigel plug assays in vivo. We here confirm that DKK1 inhibits HUVEC tubulogenesis in vitro (Min et al., 2011) and tumor angiogenesis in an osteosarcoma xenograft model in vivo.

Employing the RT2 model, we show that TNC promotes metastasis formation to the lung but not to the liver. This is reminiscent of breast cancer where TNC is part of a gene expression signature specifically associated with lung but not bone metastasis (Minn et al., 2005), an initial observation that has been subsequently confirmed and functionally validated using xenograft models (Oskarsson et al., 2011; Tavazoie et al., 2008). Mechanistically, TNC expression was linked to an increased tumor cell survival and activation of Wnt and Notch signaling, as revealed by increased expression of Lgr5 and Msi1, respectively (Oskarsson et al., 2011). Although we have shown that Wnt signaling is activated in TNC-overexpressing RT2 tumors and in cellular models comprising tumor and endothelial cells in vitro, the expression of Lgr5 and of several Notch pathway members are unaffected in the in vivo and in vitro models we used (Table S3; F.S. and G.O., unpublished data). Multiple explanations for these differences may exist, such as difference in model systems and in organ and tissue context. We have shown that the ectopic expression of TNC leads to *DKK1* downregulation and Wnt signaling activation in RT2/TNC tumors as revealed by the upregulation of other Wnt target genes, including the prototypical Wnt target *Axin2*. Conversely, in RT2/TNCKO tumors DKK1 levels were increased, but *Axin2* expression was unchanged. This result is in line with a previous report showing that the Wnt pathway has minimal basal activity in pancreatic beta tumor cells and is dispensable for RT2 tumor progression (Herzig et al., 2007). In addition to canonical Wnt signaling, the DKK1 receptor LRP6 was shown to promote PDGF-BB, TGF-β and CTGF signaling in pericytes and fibroblasts. Importantly, these signaling activities were blocked by DKK1 through binding to LRP6 (Ren et al., 2013). We suggest that a TNC-rich matrix induces a microenvironment with low DKK1 levels that is susceptible to angiogenic signaling from Wnt and other pathways regulated by DKK1. This possibility is supported by our results that have shown an inverse correlation of TNC and DKK1 expression, promotion of the angiogenic switch by TNC, and a strong downregulation of DKK1 by TNC in tumor and several stromal cell types.

In the TNC transgenic RT2 model, we observed that TNC promotes multiple early events such as proliferation and survival in hyperplastic islets, Wnt target upregulation in small, differentiated tumors, and the angiogenic switch. A major role of TNC early in tumorigenesis combined with a less functional vasculature may explain why macroscopically visible RT2 tumors of the different genotypes did not differ in size. A potential early role of TNC in tumorigenesis has not received much attention because cancer patient data with a correlation of high TNC expression and malignancy (Midwood and Orend, 2009; Oskarsson et al., 2011) rather suggested a major role of TNC in late events. In human cancer tissue, early events cannot be easily addressed, which might explain why we did not see a correlation of *TNC* and *DKK1* mRNA expression levels in human cancer tissues. TNC promotes metastasis (Minn et al., 2005; Oskarsson et al., 2011; Tavazoie et al., 2008), which has also been recapitulated here in the RT2 model and in human insulinomas where the highest TNC expression levels were observed in the few available metastatic insulinomas.

In summary, we have shown that DKK1 expression is dependent on actin stress fibers that are disrupted by TNC. We have established a transgenic immune-competent tumor mouse model that mimics the high expression of TNC observed in human cancer. Our results prove that TNC plays crucial roles along tumor progression by promoting early and late events. We demonstrate that TNC levels determine the extent of tumor cell survival, invasion, tumor angiogenesis, and metastasis. These phenotypes appear to be linked to DKK1 downregulation creating a proangiogenic tumor microenvironment. Finally, our human TNC-expressing transgenic tumor mice offer a model for human insulinoma progression and for the preclinical evaluation of drugs that target human TNC.

EXPERIMENTAL PROCEDURES

Mice

Generation of transgenic RipTNC mice, breeding, genotyping, xenograft experiments, and analysis of tumor material are specified in the Supplemental Information. RT2 mice developing pancreatic neuroendocrine tumors (Hanahan, 1985) were crossed with RipTNC (this study) or TNCKO (Forsberg et al., 1996) mice to generate double-transgenic mice with forced expression of TNC (RT2/TNC) or lacking TNC expression (RT2/TNCKO). Experiments comprising animals were performed according to the guidelines of INSERM and the Swiss Federal Veterinary Office.

Histopathological Analysis of Mouse and Human Tissue

Tumor incidence per mouse was determined as the number of all visible tumors with a minimal diameter of 1 mm. Tumor volume was calculated assuming a spherical shape with formula $V = 1/6 \times \pi \times d^3$ (d = tumor diameter). Pancreata, liver, and lung tissue were isolated, fixed in 4% paraformaldehyde (PFA) overnight followed by embedding in paraffin, fixed for 2 hr in 4% PFA, immersed in 20% sucrose overnight, and embedded in Tissue-Tek O.C.T. (Sakura Finetek) or freshly embedded in O.C.T. and frozen on dry ice.

Histological analysis was performed on 5 μm (paraffin embedded) and 7 μm (cryopreserved) tissue sections by staining with H&E or immunostaining. Primary antibodies were incubated overnight at 4°C. Immunohistochemical (IHC) detection was performed on paraffin-embedded tissue using Vectastain developing system (Vector Laboratories), followed by staining with hematoxilin. Detection by IF was performed on fixed or fresh-frozen tissue using fluorescein-isothiocyanate- or Cy3-coupled secondary antibodies (Jackson ImmunoResearch Laboratories); cell nuclei were stained with DAPI. Primary antibodies detecting the following molecules were used: phosphohistone H3 (PH3, 1:200, Upstate 06-570), cleaved caspase-3 (1:50, Cell Signaling Technology 9661), CD31 (1:50, BD Pharmingen 550274, Acris BM4086), NG2 (1:200, Millipore AB5320), insulin (1:200, Dako Cytomation A0564), glucagon (1:1000, Sigma G2654), KI67 (1:200, clone SP6, Thermo Scientific, RM-9106-S1), human TNC (BC-24, 1:3000, Sigma T2551), and fibrinogen (1:500, Dako A0080). Anti-mouse TNC MTn12 (Aufderheide and Ekblom, 1988) and anti-human TNC B28.13 antibodies (Schenk et al., 1995) were purified from hybridoma culture supernatants.

Quantification of IF microscopic pictures was done using ImageJ (National Institutes of Health) software. Staining protocols (fixation, blocking, antibody dilution) and image acquisition setting (microscope, magnification, light intensity, exposure time) were kept constant per experiment. Data were quantified

as counted events over analyzed tumor area (PH3), as area fraction over analyzed DAPI-positive cell area (cleaved caspase-3, PH3, and KI67) or as area fraction over analyzed tumor area (CD31, NG2, and fibrinogen).

Cell-Culture Experiments

Coating of cell-culture dishes with FN and TNC was performed as described earlier (Huang et al., 2001; Lange et al., 2007). Cells were seeded on the coated surfaces and analyzed using standard protocols as described. mRNA was extracted from paraffin-embedded tissue and analyzed by qRT-PCR.

Human Insulinomas

Tumor material was obtained from the Klinikum rechts der Isar (Munich, Germany) or the Hôpital de Hautepierre (Strasbourg, France). Analysis of the human insulinomas had been approved by the respective ethics committees. All samples were obtained after prior patient informed written consent. Tumor tissue was obtained from 14 patients (group 1, Munich, and group 2, Strasbourg) with endocrine pancreatic cancer and was histopathologically confirmed as insulinoma by an experienced pathologist. Presence of metastasis was diagnosed in three patients (liver or lymph node n = 2, group 1; liver and lymph node n = 1, group 2).

SUPPLEMENTAL INFORMATION

Supplemental Information includes Supplemental Experimental Procedures, seven figures, and three tables and can be found with this article online at http://dx.doi.org/10.1016/j.celrep.2013.09.014.

ACKNOWLEDGMENTS

We thank W. Huang, A.-C. Feutz, K. Strittmatter, H. Antoniadis, P. Lorentz, M.-F. Hamou, B. Scolari, R. Buergy, E. Domany, J. Huelsken, R. Fässler, M. Kedinger, I. Gross, G. Posern, R. Moon, and R. Chiquet-Ehrismann for technical assistance, reagents, mice, discussion, and help with the generation of the transgenic mice. Support was generously provided by the University Strasbourg and the Association pour la Recherche sur le cancer (to A.S.); the Fondation des Treilles (to F.S.); INSERM/Region Alsace (to I.G.); the Ligue contre le Cancer (to O.L., P.S.-A., and G.O.); and INSERM, University Strasbourg, Agence National de la Recherche, Krebsliga Beider Basel, the Association for International Cancer Research, the Swiss National Science Foundation, Oncosuisse, the Novartis Foundation for Biological and Medical Sciences, the Hôpital de Hautepierre, the Association pour la Recherche contre le Cancer, and the Institut National du Cancer (to G.O.).

Received: March 20, 2013
Revised: August 7, 2013
Accepted: September 10, 2013
Published: October 17, 2013

REFERENCES

Aguilera, O., Fraga, M.F., Ballestar, E., Paz, M.F., Herranz, M., Espada, J., García, J.M., Muñoz, A., Esteller, M., and González-Sancho, J.M. (2006). Epigenetic inactivation of the Wnt antagonist DICKKOPF-1 (DKK-1) gene in human colorectal cancer. Oncogene *25*, 4116–4121.

Aguirre-Ghiso, J.A. (2007). Models, mechanisms and clinical evidence for cancer dormancy. Nat. Rev. *7*, 834–846.

Aicher, A., Kollet, O., Heeschen, C., Liebner, S., Urbich, C., Ihling, C., Orlandi, A., Lapidot, T., Zeiher, A.M., and Dimmeler, S. (2008). The Wnt antagonist Dickkopf-1 mobilizes vasculogenic progenitor cells via activation of the bone marrow endosteal stem cell niche. Circ. Res. *103*, 796–803.

Almog, N. (2010). Molecular mechanisms underlying tumor dormancy. Cancer Lett. *294*, 139–146.

Aufderheide, E., and Ekblom, P. (1988). Tenascin during gut development: appearance in the mesenchyme, shift in molecular forms, and dependence on epithelial-mesenchymal interactions. J. Cell Biol. *107*, 2341–2349.

Barbolina, M.V., Liu, Y., Gurler, H., Kim, M., Kajdacsy-Balla, A.A., Rooper, L., Shepard, J., Weiss, M., Shea, L.D., Penzes, P., et al. (2013). Matrix rigidity activates Wnt signaling through down-regulation of Dickkopf-1 protein. J. Biol. Chem. *288*, 141–151.

Bass, M.D., and Humphries, M.J. (2002). Cytoplasmic interactions of syndecan-4 orchestrate adhesion receptor and growth factor receptor signalling. Biochem. J. *368*, 1–15.

Bissell, M.J., and Labarge, M.A. (2005). Context, tissue plasticity, and cancer: are tumor stem cells also regulated by the microenvironment? Cancer Cell *7*, 17–23.

Chiquet-Ehrismann, R., Mackie, E.J., Pearson, C.A., and Sakakura, T. (1986). Tenascin: an extracellular matrix protein involved in tissue interactions during fetal development and oncogenesis. Cell *47*, 131–139.

De Langhe, S.P., Sala, F.G., Del Moral, P.M., Fairbanks, T.J., Yamada, K.M., Warburton, D., Burns, R.C., and Bellusci, S. (2005). Dickkopf-1 (DKK1) reveals that fibronectin is a major target of Wnt signaling in branching morphogenesis of the mouse embryonic lung. Dev. Biol. *277*, 316–331.

De Laporte, L., Rice, J.J., Tortelli, F., and Hubbell, J.A. (2013). Tenascin C promiscuously binds growth factors via its fifth fibronectin type III-like domain. PLoS ONE *8*, e62076.

Forsberg, E., Hirsch, E., Fröhlich, L., Meyer, M., Ekblom, P., Aszodi, A., Werner, S., and Fässler, R. (1996). Skin wounds and severed nerves heal normally in mice lacking tenascin-C. Proc. Natl. Acad. Sci. USA *93*, 6594–6599.

Gineitis, D., and Treisman, R. (2001). Differential usage of signal transduction pathways defines two types of serum response factor target gene. J. Biol. Chem. *276*, 24531–24539.

Glinka, A., Wu, W., Delius, H., Monaghan, A.P., Blumenstock, C., and Niehrs, C. (1998). Dickkopf-1 is a member of a new family of secreted proteins and functions in head induction. Nature *391*, 357–362.

Hanahan, D. (1985). Heritable formation of pancreatic beta-cell tumours in transgenic mice expressing recombinant insulin/simian virus 40 oncogenes. Nature *315*, 115–122.

Hanahan, D., and Folkman, J. (1996). Patterns and emerging mechanisms of the angiogenic switch during tumorigenesis. Cell *86*, 353–364.

Hanahan, D., Christofori, G., Naik, P., and Arbeit, J. (1996). Transgenic mouse models of tumour angiogenesis: the angiogenic switch, its molecular controls, and prospects for preclinical therapeutic models. Eur. J. Cancer *32A*, 2386–2393.

Herzig, M., Savarese, F., Novatchkova, M., Semb, H., and Christofori, G. (2007). Tumor progression induced by the loss of E-cadherin independent of beta-catenin/Tcf-mediated Wnt signaling. Oncogene *26*, 2290–2298.

Huang, W., Chiquet-Ehrismann, R., Moyano, J.V., Garcia-Pardo, A., and Orend, G. (2001). Interference of tenascin-C with syndecan-4 binding to fibronectin blocks cell adhesion and stimulates tumor cell proliferation. Cancer Res. *61*, 8586–8594.

Huijbers, E.J., Ringvall, M., Femel, J., Kalamajski, S., Lukinius, A., Abrink, M., Hellman, L., and Olsson, A.K. (2010). Vaccination against the extra domain-B of fibronectin as a novel tumor therapy. FASEB J. *24*, 4535–4544.

Kerbel, R.S. (2008). Tumor angiogenesis. N. Engl. J. Med. *358*, 2039–2049.

Lange, K., Kammerer, M., Hegi, M.E., Grotegut, S., Dittmann, A., Huang, W., Fluri, E., Yip, G.W., Götte, M., Ruiz, C., and Orend, G. (2007). Endothelin receptor type B counteracts tenascin-C-induced endothelin receptor type A-dependent focal adhesion and actin stress fiber disorganization. Cancer Res. *67*, 6163–6173.

Lange, K., Kammerer, M., Saupe, F., Hegi, M.E., Grotegut, S., Fluri, E., and Orend, G. (2008). Combined lysophosphatidic acid/platelet-derived growth factor signaling triggers glioma cell migration in a tenascin-C microenvironment. Cancer Res. *68*, 6942–6952.

Levental, K.R., Yu, H., Kass, L., Lakins, J.N., Egeblad, M., Erler, J.T., Fong, S.F., Csiszar, K., Giaccia, A., Weninger, W., et al. (2009). Matrix crosslinking forces tumor progression by enhancing integrin signaling. Cell *139*, 891–906.

Liao, Y.L., Sun, Y.M., Chau, G.Y., Chau, Y.P., Lai, T.C., Wang, J.L., Horng, J.T., Hsiao, M., and Tsou, A.P. (2008). Identification of SOX4 target genes using phylogenetic footprinting-based prediction from expression microarrays suggests that overexpression of SOX4 potentiates metastasis in hepatocellular carcinoma. Oncogene *27*, 5578–5589.

Lu, P., Weaver, V.M., and Werb, Z. (2012). The extracellular matrix: a dynamic niche in cancer progression. J. Cell Biol. *196*, 395–406.

Menezes, M.E., Mitra, A., Shevde, L.A., and Samant, R.S. (2012). DNAJB6 governs a novel regulatory loop determining Wnt/β-catenin signalling activity. Biochem. J. *444*, 573–580.

Metz, D.C., and Jensen, R.T. (2008). Gastrointestinal neuroendocrine tumors: pancreatic endocrine tumors. Gastroenterology *135*, 1469–1492.

Midwood, K.S., Valenick, L.V., Hsia, H.C., and Schwarzbauer, J.E. (2004). Coregulation of fibronectin signaling and matrix contraction by tenascin-C and syndecan-4. Mol. Biol. Cell *15*, 5670–5677.

Midwood, K.S., and Orend, G. (2009). The role of tenascin-C in tissue injury and tumorigenesis. J. Cell Commun. Signal *3*, 287–310.

Midwood, K.S., Hussenet, T., Langlois, B., and Orend, G. (2011). Advances in tenascin-C biology. Cell. Mol. Life Sci. *68*, 3175–3199.

Mills, G.B., and Moolenaar, W.H. (2003). The emerging role of lysophosphatidic acid in cancer. Nat. Rev. *3*, 582–591.

Min, J.K., Park, H., Choi, H.J., Kim, Y., Pyun, B.J., Agrawal, V., Song, B.W., Jeon, J., Maeng, Y.S., Rho, S.S., et al. (2011). The WNT antagonist Dickkopf2 promotes angiogenesis in rodent and human endothelial cells. J. Clin. Invest. *121*, 1882–1893.

Minn, A.J., Kang, Y., Serganova, I., Gupta, G.P., Giri, D.D., Doubrovin, M., Ponomarev, V., Gerald, W.L., Blasberg, R., and Massagué, J. (2005). Distinct organ-specific metastatic potential of individual breast cancer cells and primary tumors. J. Clin. Invest. *115*, 44–55.

Miralles, F., Posern, G., Zaromytidou, A.I., and Treisman, R. (2003). Actin dynamics control SRF activity by regulation of its coactivator MAL. Cell *113*, 329–342.

Murphy-Ullrich, J.E., Lightner, V.A., Aukhil, I., Yan, Y.Z., Erickson, H.P., and Höök, M. (1991). Focal adhesion integrity is downregulated by the alternatively spliced domain of human tenascin. J. Cell Biol. *115*, 1127–1136.

Nevins, J.R. (2001). The Rb/E2F pathway and cancer. Hum. Mol. Genet. *10*, 699–703.

Oh, H., Ryu, J.H., Jeon, J., Yang, S., Chun, C.H., Park, H., Kim, H.J., Kim, W.S., Kim, H.H., Kwon, Y.G., and Chun, J.S. (2012). Misexpression of Dickkopf-1 in endothelial cells, but not in chondrocytes or hypertrophic chondrocytes, causes defects in endochondral ossification. J. Bone Miner. Res. *27*, 1335–1344.

Orend, G., Huang, W., Olayioye, M.A., Hynes, N.E., and Chiquet-Ehrismann, R. (2003). Tenascin-C blocks cell-cycle progression of anchorage-dependent fibroblasts on fibronectin through inhibition of syndecan-4. Oncogene *22*, 3917–3926.

Oskarsson, T., Acharyya, S., Zhang, X.H., Vanharanta, S., Tavazoie, S.F., Morris, P.G., Downey, R.J., Manova-Todorova, K., Brogi, E., and Massagué, J. (2011). Breast cancer cells produce tenascin C as a metastatic niche component to colonize the lungs. Nat. Med. *17*, 867–874.

Parangi, S., O'Reilly, M., Christofori, G., Holmgren, L., Grosfeld, J., Folkman, J., and Hanahan, D. (1996). Antiangiogenic therapy of transgenic mice impairs de novo tumor growth. Proc. Natl. Acad. Sci. USA *93*, 2002–2007.

Pendás-Franco, N., Aguilera, O., Pereira, F., González-Sancho, J.M., and Muñoz, A. (2008). Vitamin D and Wnt/beta-catenin pathway in colon cancer: role and regulation of DICKKOPF genes. Anticancer Res. *28*(5A), 2613–2623.

Pipas, J.M., and Levine, A.J. (2001). Role of T antigen interactions with p53 in tumorigenesis. Semin. Cancer Biol. *11*, 23–30.

Reis, M., Czupalla, C.J., Ziegler, N., Devraj, K., Zinke, J., Seidel, S., Heck, R., Thom, S., Macas, J., Bockamp, E., et al. (2012). Endothelial Wnt/β-catenin signaling inhibits glioma angiogenesis and normalizes tumor blood vessels by inducing PDGF-B expression. J. Exp. Med. *209*, 1611–1627.

Ren, S., Johnson, B.G., Kida, Y., Ip, C., Davidson, K.C., Lin, S.L., Kobayashi, A., Lang, R.A., Hadjantonakis, A.K., Moon, R.T., and Duffield, J.S. (2013). LRP-6 is a coreceptor for multiple fibrogenic signaling pathways in pericytes and myofibroblasts that are inhibited by DKK-1. Proc. Natl. Acad. Sci. USA *110*, 1440–1445.

Ruiz, C., Huang, W., Hegi, M.E., Lange, K., Hamou, M.F., Fluri, E., Oakeley, E.J., Chiquet-Ehrismann, R., and Orend, G. (2004). Growth promoting signaling by tenascin-C [corrected]. Cancer Res. *64*, 7377–7385.

Schenk, S., Muser, J., Vollmer, G., and Chiquet-Ehrismann, R. (1995). Tenascin-C in serum: a questionable tumor marker. Int. J. Cancer *61*, 443–449.

Smadja, D.M., d'Audigier, C., Weiswald, L.B., Badoual, C., Dangles-Marie, V., Mauge, L., Evrard, S., Laurendeau, I., Lallemand, F., Germain, S., et al. (2010). The Wnt antagonist Dickkopf-1 increases endothelial progenitor cell angiogenic potential. Arterioscler. Thromb. Vasc. Biol. *30*, 2544–2552.

Song, S., Ewald, A.J., Stallcup, W., Werb, Z., and Bergers, G. (2005). PDGFRbeta+ perivascular progenitor cells in tumours regulate pericyte differentiation and vascular survival. Nat. Cell Biol. *7*, 870–879.

Spencer, J.A., and Misra, R.P. (1999). Expression of the SRF gene occurs through a Ras/Sp/SRF-mediated-mechanism in response to serum growth signals. Oncogene *18*, 7319–7327.

Tanaka, K., Hiraiwa, N., Hashimoto, H., Yamazaki, Y., and Kusakabe, M. (2004). Tenascin-C regulates angiogenesis in tumor through the regulation of vascular endothelial growth factor expression. Int. J. Cancer *108*, 31–40.

Tavazoie, S.F., Alarcón, C., Oskarsson, T., Padua, D., Wang, Q., Bos, P.D., Gerald, W.L., and Massagué, J. (2008). Endogenous human microRNAs that suppress breast cancer metastasis. Nature *451*, 147–152.

van Obberghen-Schilling, E., Tucker, R.T., Saupe, F., Gasser, I., Cseh, B., and Orend, G. (2011). Fibronectin and tenascin-C: accomplices in vascular morphogenesis during development and tumor growth. Int. J. Dev. Biol. *55*, 511–525.

Wenk, M.B., Midwood, K.S., and Schwarzbauer, J.E. (2000). Tenascin-C suppresses Rho activation. J. Cell Biol. *150*, 913–920.

Wu, F.T., Stefanini, M.O., Mac Gabhann, F., and Popel, A.S. (2009). A compartment model of VEGF distribution in humans in the presence of soluble VEGF receptor-1 acting as a ligand trap. PLoS ONE *4*, e5108.

Zhou, A.D., Diao, L.T., Xu, H., Xiao, Z.D., Li, J.H., Zhou, H., and Qu, L.H. (2012). β-Catenin/LEF1 transactivates the microRNA-371-373 cluster that modulates the Wnt/β-catenin-signaling pathway. Oncogene *31*, 2968–2978.